DOI 10.5162/sensoren2024/P14

Improving sensor performance of gas sensors by micropumps

Oliver Zett[1,2], *Michael Henfling*[1,2], *Agnes Bußmann*[1]
[1] *Fraunhofer Institute for Electronic Microsystems and Solid State Technologies EMFT*
Hansastraße 27 d, 80686 Munich, Germany
[2] *Universität der Bundeswehr München*
Werner-Heisenberg-Weg 39, 85579 Neubiberg, Germany

Abstract

The detection of different gases is required in many technical applications or safety relevant devices. The detection threshold, accuracy and response time are often limited and insufficient for demanding applications. To increase sensor performance, increased pressure can be beneficial. In this publication we demonstrate the combination of a commercially available CO_2 sensor that uses the photoacoustic NDIR sensing principle and a micro diaphragm pump fabricated by Fraunhofer EMFT. Several possible advantages result from this combination: improved response times, wider detection limits concerning the upper and lower limit, actual volumetric measurements and sharper temporal resolution. We use a custom made measurement setup and a reference system to validate these claims. Our results show a shift of the sensor signal by over 40% when increasing the pressure in the measurement chamber by 200 mbar with a micropump. We also observed a signal reduction of over 30% when reducing the pressure by 200 mbar with a micropump. These intentional signal shifts can also be achieved with sensors working with different sensing principles due to the physics of the ideal gas law. Furthermore, we show an improved response time. In future the different configurations that we tested in this study will be combined into one configuration. In addition, smaller micropumps from Fraunhofer EMFT can reduce the overall system size significantly. The resulting measurement unit can address challenging applications in gas sensing, due to the improved sensor performance.

Keywords: CO_2 sensor, micropump, sensor improvement, active sampling

Introduction

There is a wide range of monitoring applications that require gas sensors for various gases. A low detection threshold is crucial for many of those applications, especially in the case of safety relevant devices, where the target gas is harmful to health. There are two ways to improve the lower detection threshold. Either current sensor technology itself can be improved or an active sampling and compression of the target gas can increase the sensitivity.
Active sampling in combination with compression is challenging if the available space is limited, since miniaturized fluidic actuators and microfluidic channels are necessary. In this contribution we propose the combination of piezoelectrically driven micro diaphragm pumps, see Fig. 1, with gas sensors to improve the system performance in various regards while remaining small and portable. Active sampling and compressing has several advantages including faster response times and an increased working range of a gas sensor. The latter can be explained utilizing the ideal gas law depicted below, see equation 1.

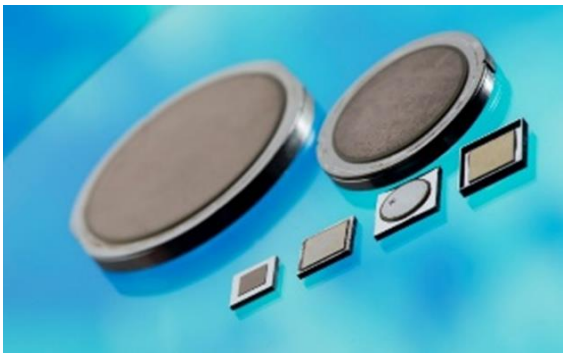

Fig. 1 Portfolio of the Fraunhofer EMFT micropumps. The cuboid shaped micropumps are manufactured with photolithography methods, while the cylindrical shaped micropumps are fabricated with a laser welding process.

Due to a change in pressure, the number of molecules per volume and thus the density of the gas changes. This relationship has a

significant impact on the measurement result. With this approximation, we expect a linear behavior of the sensors signal: A pressure change of Δp = ± 200 mbar results in a signal change of ± 20%, compared to the signal at 1000 mbar [1]. With the micro diaphragm pumps it is possible to control the gas pressure as well as the gas volume that passes through the sensor.

$$p \times V = n \times R \times T \qquad (1)$$

p: Gas pressure
V: Gas volume
n: Amount of substance
R: Universal gas constant
T: Gas temperature

Materials and Methods

The following paragraphs describe the measurement setup and which equipment was used to derive the measurements.

Micropumps

Micropumps come in a wide variety of geometries and operating principles [2]. A research group of the Fraunhofer EMFT specializes in micropumps that can be categorized as displacement pumps with piezoelectric bending actuators and passive check valves. A portfolio of Fraunhofer EMFTs micropumps reaching from the world's smallest micro diaphragm pump with an edge length of 3.5 mm to a micropump with a diameter of 30 mm is depicted in Fig. 1. The micropump utilized in this work (second largest pump in Fig. 1) is made from stainless steel and has an outer diameter of 20 mm with a chamber diameter of 18 mm and a chamber height of approximately 60 µm. It is actuated with an alternating signal, e.g., sinusoidal or square wave signal form, reaching from -80 V to 300 V. The asymmetrical actuation signal results from the induced pretension during the piezo mounting process and polarized piezoelectric ceramic [4]. Fig. 2 illustrates the pretension of the micropump in the initial state and its working principle.

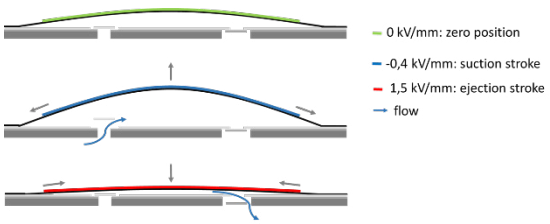

Fig. 2 A cross section of a micropump in its initial state (top), during suction stroke (middle) and during ejection stoke (bottom).

Measurement Setup

To test our hypothesis, we utilize two sensor nodes that each contain two commercially available sensors: a CO_2 Sensor from Sensirion (SDC41) that uses the photoacoustic NDIR sensing principle, and a Multiparameter sensor from Bosch (BME680) that measures humidity, temperature, pressure and VOCs. All sensors were operated in a standard configuration. For the SDC41 the auto calibration was disabled. For readout of the SDC41 sensors we used the SEK-SensorBridge and ControlCenter Software from Sensirion. For the BME680, two Arduino Uno microcontroller boards and serial I2C connections were used. One sensor node is placed in a stainless-steel measurement chamber with an inner volume of 250 ml to simulate ambient conditions. The other sensor node is placed outside of the measurement chamber and is housed in a gas tight 3D-printed flow cell. The flow cell material is out of clear resin from Formlabs with a volume of 11 cm^3. The flow cell is directly connected to the measurement chamber by two 30 cm long silicone tubes with an inner diameter of 2 mm from Deutsch & Neumann GmbH. For the generation of different CO_2 concentrations, a premixed test gas of 5% CO_2 in synthetic air and synthetic air as the carrier gas were purchased from Linde AG. To ensure the correct CO_2 concentration and humidity of the test gas, the gas mixer HovaCAL® 7836-VOC from IAS GmbH Germany was used. To generate a constant pressure in the measurement chamber and throughout the entire system a custom-built pressure regulation system was implanted. This system consists of a 1:1 dome-loaded back pressure regulator LF series from Equilibar. The pilot pressure is set using the Bronkhorst ERC Series ERC-1C-001.6PA electronic pressure regulator. The pressure within the measurement chamber can be adjusted within a range of 700 mbar to 1200 mbar. The absolute pressure inside the measurement chamber is recorded by a precision pressure sensor FDAD 35-M00 from Ahlborn. To determine the flow rate of the micro pump, the flow meter EL-Flow Prestige FG-111B from Bronkhorst was used. To adjust dynamic pressure as well as the flow through the flow cell a common needle valve was used, see Fig. 3.

Sensor system Characterization

A piezoelectric micro diaphragm pump with passive ortho-planar valves was used for the experiments. This pump was developed at

Fraunhofer EMFT [3]. It has a diameter of 20 mm and a height of 1.5 mm. The pump can create overpressure of over 400 mbar and negative pressure of more than 200 mbar. This pressure range enables an increase of a sensor's measurement range. A manual needle valve is used to control the pressure build up in the sensor nodes flow cell. A positive or negative pressure of 200 mbar in the flow cell is achieved while maintaining a flowrate of multiple ml/min with this approach.

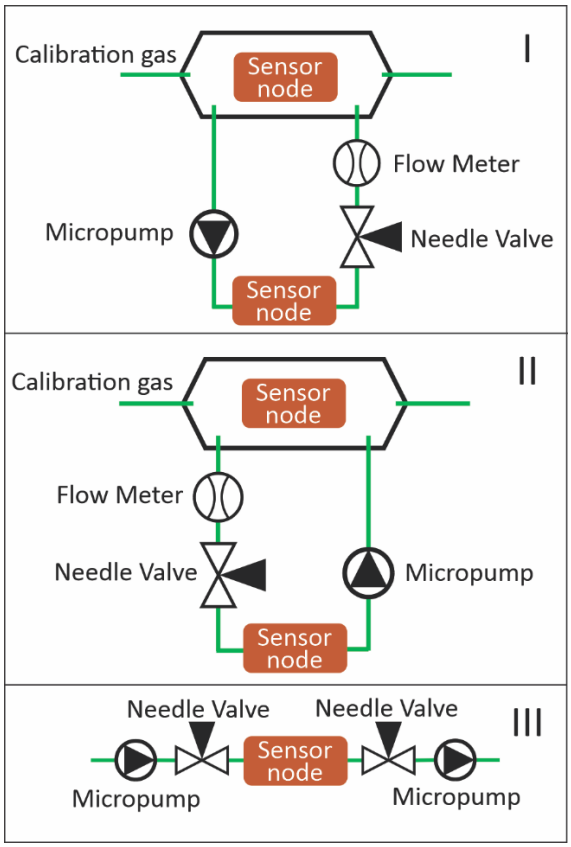

Fig. 3 Different measurement setups are depicted. Setups I and II are part of the experiments while setup III envisions the future pneumatic actuator unit.

We conduct our experiments with a set of two sensor nodes for comparing purposes. One sensor is set into the direct downstream of the test gas, which is provided by our gas mixer, the other is connected in parallel with a micropump and a valve in series. Fig. 3 shows the two different setups (setup I and setup II) which were examined. Setup I generates a positive pressure by a restricted needle valve. Setup II generates a negative pressure by a restricted needle valve. Both setups also simulate sampling tubes and their influence on the response time and senor performance.
The III configuration shows the pneumatic actuator that we are going to develop for optimal sensor improvement. It allows the operation in both above-mentioned setups. The long scope is to implement a pneumatic actuator unit that can be combined with various gas sensors to enhance their capabilities.

Results

The SCD41 and the micropump are characterized individually, before the two setups, combining micropump and gas sensor, are tested.

Sensor Characterization

The first measurement shows the behavior of the SDC41 at different atmospheric pressures from 700 mbar to 1200 mbar, see Fig. 4. For this experiment, the CO_2 concentration, temperature and the abs. humidity were constantly set to 2000 ppm CO_2, 20 °C and 1 % abs. humidity.

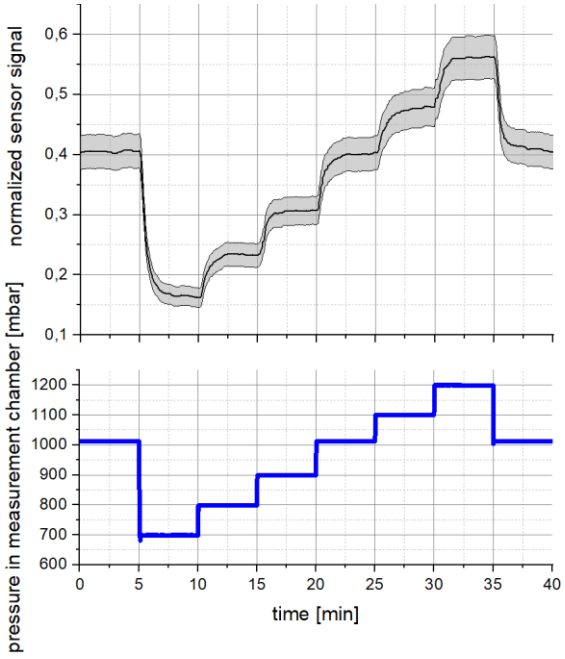

Fig. 4 Pressure calibration at 2000 ppm CO_2 ,20 °C and 1% abs. humidity with 1013 mbar, 700 mbar, 800 mbar, 900 mbar, 1013 mbar, 1100 mbar, 1200 mbar and 1013 mbar.

Based on this pressure dependency where the sensor shows higher CO_2 values at higher pressure and lower CO_2 values at lower pressure, we can now manipulate the pressure in the flow cell. It also shows that the sensor does not adhere precisely to the ideal gas equation, which is to be expected considering the complexities and deviations present in real-world gas measurements.

Micropump Characterization

For the characterization of the micropump a profilometer Fries Research & Technology MircroProf, a waveform generator Agilent Keysight 33500B, a signal amplifier Piezomechanik SVR150/3, a flow sensor EL-Flow Prestige FG-111B from Bronkhorst and a pressure controller CPC 3000 from Mensor were used. An initial characterization of the micropump illustrates the best operating conditions and its expected performance.

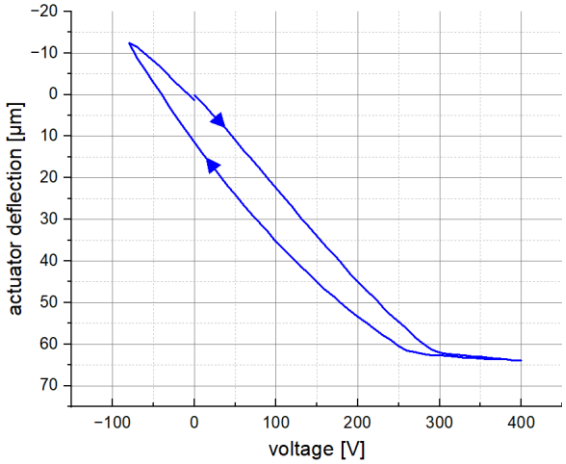

Fig. 5 Static displacement measurement of the micropump. The displacement is measured at the center of the micropump while a voltage sweep is applied to the piezoelectric bending actuator.

Fig. 5 displays the static deflection measured at the center of the micropump depending on the applied voltage. The curve depicted has a typical hysteresis, that is caused by the piezoelectric nature of the actuator, as described in earlier publications [3]. The slope of the graph is significantly decreased between 300 V and 400 V. This change in slope is caused by a touchdown of the diaphragm to the pump chamber bottom, which blocks any further downwards movement. The touchdown allows the diaphragm to move very far towards the chamber bottom und thus reduces the residual dead volume in the chamber after the ejection stroke. This reduced dead volume leads to a good compression ratio and therefore beneficial air transport properties. Based on the actuator stroke measurement, we choose an actuation amplitude of 300 V and –80 V ss peak values for flow rate characterization of the pump.

The backpressure capability refers to the ability of the micropump to overcome resistance or pressure in the fluidic system. In Fig. 6, the micropump was tested under increasing levels of backpressure until 0 ml/min flow is detected. Two actuation signal forms were tested: a sinusoidal signal (blue curve) and a square wave signal (orange curve). The micropump shows a high backpressure capability of over 300 mbar when actuated with a sinusoidal waveform and an even higher capability of over 400 mbar when a square wave signal is applied. The higher pressure capability with rectangular actuation is caused by the faster actuator movement. This fast change of volume in the chamber causes a rapid pressure increase and leads to a higher absolute pressure in the chamber. Additionally, the fast pressure change leads to fast valve opening and closing, leading to better effective fluid flow.

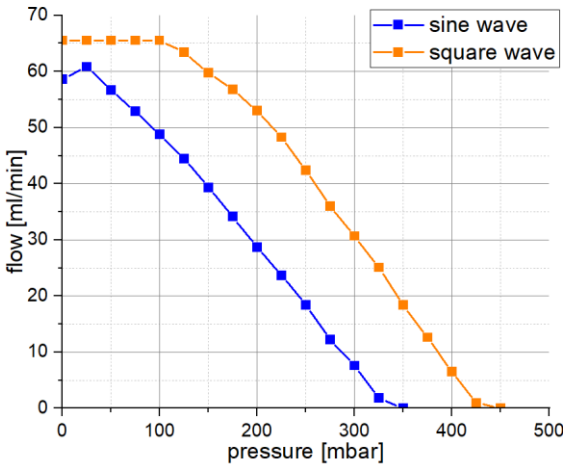

Fig. 6 The backpressure capability of the micropump is depicted. A 250 Hz signal with peak values of 300 V and –80 V is applied. The pressure against the micropumps pumping direction was increased until no flow is detected anymore. The measurement was performed with two signal forms.

Combination of Gas Sensor and Micropump

To investigate the influence of the micropump on the gas sensor, the micropump was operated at different frequencies and installed before and after the sensor node in overpressure setup I and negative pressure setup II. The humidity, temperature and CO_2 concentration in the measurement chamber were kept constant at 1% absolute humidity, 20 °C and 2000 ppm CO_2. In setup I, the micropump was driven with a sinusoidal signal form at 10 Hz, 73 Hz, and 250 Hz. The needle valve was adjusted at 250 Hz to generate an overpressure of 1200 mbar. Corresponding to that needle valve position, the other frequencies were adjusted to generate 1100 mbar (at 73 Hz) and 1025 mbar at 10 Hz. Fig. 7 shows the sensor signals of the reference sensor and the sensor with the micropump. It clearly shows that the sensor signal of the sensor with the

micropump fluctuates at 10 Hz. We assume that the SCD41, especially on account of the NDIR sensing principle, picks up on the pressure pulses given by the micropump for lower frequencies in this case 10 Hz, whereas at 73 Hz and 250 Hz, the sensor signal stays constant and stable. Due to the pressure increase, the sensor signal of the sensor with the micropump is shifted to higher values compared to the reference sensor.

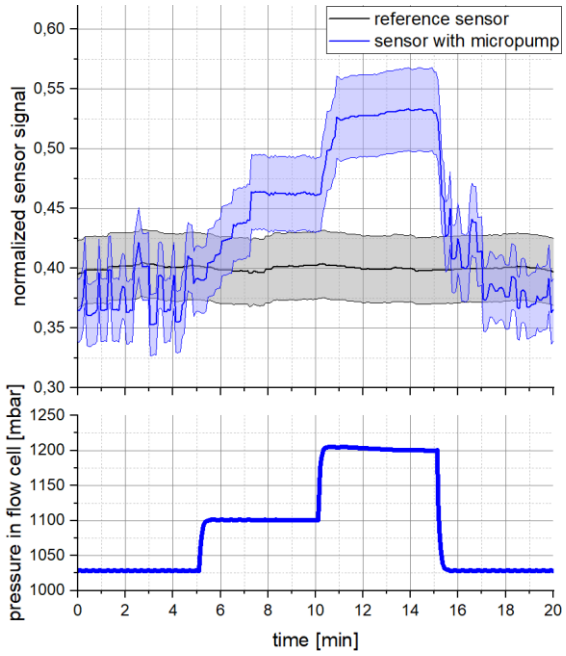

Fig. 7 Measurement in setup I of the CO_2 sensor reaction (upper graph) to a micropump generating 100 mbar and 200 mbar overpressure (lower graph). The blue and black areas show the sensor inaccuracy taken from the datasheet (±40 ppm plus 5% of the sensor value).

Fig. 8 shows the results of the frequency changes in negative pressure setup II. Here, the frequencies of 10 Hz, 53 Hz, and 250 Hz were used. The needle valve was partially closed to achieve a pressure of 800 mbar at 250 Hz. At frequencies of 10 Hz and 53 Hz, pressures of 980 mbar and 900 mbar were reached utilizing a sinusoidal signal form. At 10 Hz, the sensor with the micropump shows similar fluctuations as seen for overpressure measurements depicted in Fig. 7. At 53 Hz, this signal begins to oscillate with a higher amplitude. At 250 Hz, this signal stays stable and constant but at a lower value compared to the reference sensor, due to the pressure reduction.

The sensitivity of the sensor was influenced by the micropump through different settings. For the overpressure setup I, the micropump was driven with a sinusoidal signal at 250 Hz with a regulated flow of around 30 ml/min. The sinusoidal signal form was chosen, although a square wave signal is capable of higher flow rates and backpressures, to reduce pressure pluses which increase with the actuation signal's slope. In this experiment, the CO_2 concentration was changed, in 10-minute intervals, from 0 ppm, 200 ppm, 400 ppm, 600 ppm, 2000 ppm, and then in reverse until the original concentration of 0 ppm was reached.

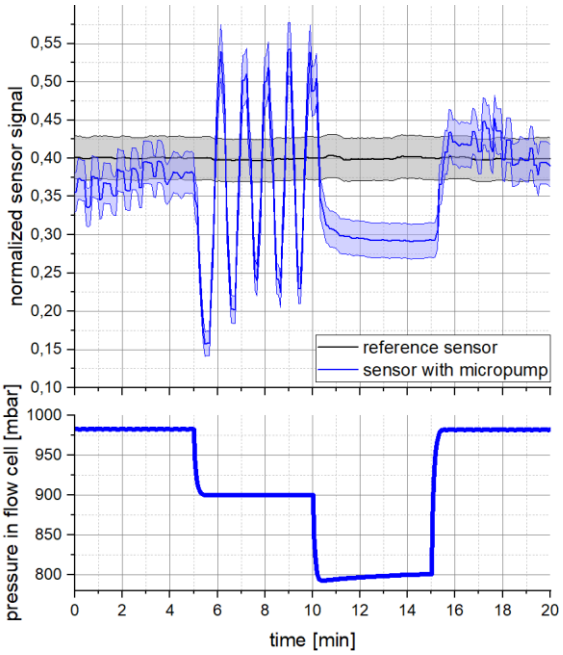

Fig. 8 Measurement in setup II of the CO_2 sensor reaction (upper graph) to a micropump generating 100 mbar and 200 mbar negative pressure (lower graph). Oscillations can be observed at the 100 mbar negative pressure due to a certain frequency (53 Hz) with which the micropump was actuated. The blue and black areas show the sensor inaccuracy taken from the datasheet (±40 ppm plus 5% of the sensor value).

For the negative pressure setup II, the CO_2 concentration was changed, in 10-minute intervals, from 2000 ppm, 3000 ppm, 4000 ppm, 5000 ppm, 6000 ppm, and then in reverse until the original concentration of 2000 ppm was reached. Also 250 Hz and a sinusoidal signal form were applied to the micropump during this measurement. This resulted in a flow rate of around 20 ml/min.

The results in Fig. 9 and Fig. 10 show the expected signal behavior in response to the deployed pressure. For the overpressure setup I, the signal values differ in the arithmetic mean by over 40% compared to the reference sensor

towards higher values. For the negative pressure setup II, the signal value changed in the arithmetic mean by 30% compared to the reference sensor towards lower values.

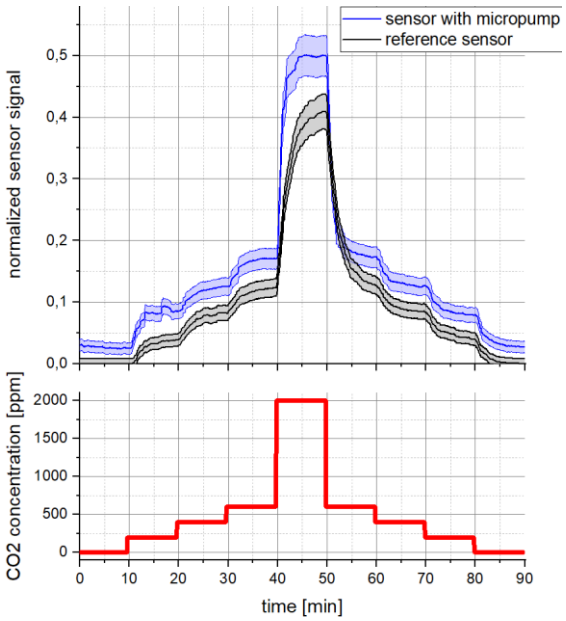

Fig. 9 Sensor responses of the SDC41 atmospheric condition in black and of the negative pressure setup II in blue.

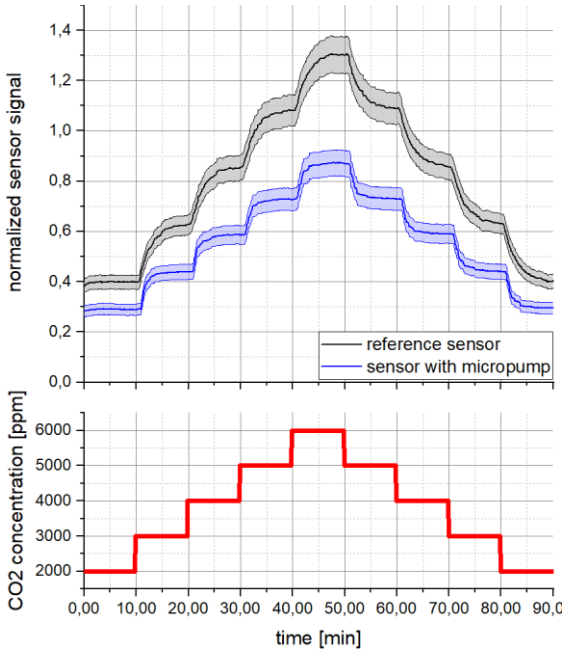

Fig. 10 Sensor responses of the SDC41 atmospheric condition in black and of the over pressure setup I in blue.

Discussion and Future Scope

The results shown emphasize the benefits as well as the technical challenges that come with the integration of a micropump with a photoacoustic NDIR sensing-based CO_2 sensor. Due to the pulse rates produced by the micropump, the frequencies can have a significant impact on the measurement stability. Particularly for lower frequencies and in the negative pressure setup, the sensor exhibits fluctuating signals that oscillate highly. For higher frequencies, we observed more stable signals of the CO_2 sensor. Therefore, higher frequencies can be used to apply over pressure and negative pressure to the sensor node. In our sensor setup the SCD 41 shows a higher impact for the pressure dependency as suggested by the ideal gas equation.
More investigations on the combination of micropumps with gas sensors need to be conducted. It is important to assess how the accuracy of the sensor is affected by a micropump.
A fully integrated system, as shown in setup III Fig. 3 with silicon micropumps and valves from Fraunhofer EMFT, needs to be built and characterized with additional measurements concerning pressure pulses generated by the micropump. Therefore, a pressure sensor with a high measurement frequency needs to be incorporated into the flow cell. Also, gas sensors with other working principles need to be evaluated. With an active control of the pressure inside a gas sensor it would be possible to implement the pressure dependency as a useful tool not only to improve the sensitivity but also other aspects such as: response time, recovery time, sensor regeneration processes as well as sensing in high altitudes or harsh environments where a normal pressure compensation is no longer applicable.

References

[1] Wiegleb, G. (2016). Gasmesstechnik in Theorie und Praxis: Messgeräte, Sensoren, Anwendungen. Springer-Verlag.
[2] Bußmann, A. B., Grünerbel, L. M., Durasiewicz, C. P., Thalhofer, T. A., Wille, A., & Richter, M. (2021). Microdosing for drug delivery application—A review. Sensors and Actuators A: Physical, 330, 112820.
[3] Bußmann, A. B., Durasiewicz, C. P., Kibler, S. H. A., & Wald, C. K. (2021). Piezoelectric titanium based microfluidic pump and valves for implantable medical applications. Sensors and Actuators A: Physical, 323, 112649.
[4] Herz, M., Richter, M., & Wackerle, M. (2016). U.S. Patent No. 9,410,641. Washington, DC: U.S. Patent and Trademark Office.